

DOI: 10.1002/elan.201900225

Protein-film Voltammetry of Two-step Electrode Enzymatic Reactions Coupled with an Irreversible Chemical Reaction of a Final Product—a Theoretical Study in Square-wave Voltammetry

Pavlinka Kokoskarova,^[a] Viktorija Maksimova,^[a] Milkica Janeva,^[a] and Rubin Gulaboski*^[a]

Abstract: Redox mechanisms in which a consecutive two-step electrode transformation occurs, and the product generated in the second electrochemical step at the electrode surface is coupled to a follow-up irreversible chemical reaction, is theoretically considered under conditions of square-wave voltammetry. The electrochemical description of considered systems is a “surface EECirr mechanism”. With the methodology named “protein-film square-wave voltammetry” we provide theoretical information on kinetics and thermodynamics of many lipophilic enzymes containing quinones or polyvalent cations of transient metals as redox active sites. We address theoretically situations of energetically separated square-

wave voltammetric peaks for at least -150 mV at potential scale. We also consider also a complex scenario of a single voltammetric peak, hiding in its shape both the features of electrode steps (occurring at same potential) and the chemical reaction. We pay a particular attention on how to distinguish the surface two-step EECirr mechanism from a simple one-step surface ECirr mechanism, but also from other two-step surface mechanisms. While presenting plenty of calculated square-wave voltammograms relevant to many enzymatic systems, we point out several simple features that allow kinetic characterization of studied mechanism from time-independent experiments at constant scan rate.

Keywords: two-step electrode mechanisms · protein-film voltammetry · surface EECirreversible mechanism · kinetics of chemical and electrode reactions · ECirreversible mechanism

1. Introduction

Experimental electrochemistry on so-called “redox enzymes” got significantly boosted in the last 20 years, mainly driven by the methodology named as “protein-film voltammetry” proposed by Armstrong et al [1–5]. When performing electrochemical experiments with redox enzymes in solutions, problems are always met that arise mainly from adsorption phenomena and irreversible denaturation processes of the redox enzymes at the working electrode surface [1,6]. In that respect, the “protein-film voltammetry” made significant improvement in performing electrochemistry on many redox enzymes [1,5–7]. This methodology relies on voltammetric experiments performed with minute amount of given redox enzyme, uniformly adsorbed at the working electrode surface. Such modified, the working electrode is subsequently submerged in electrolyte solution containing defined substrate, and common voltammetric experiments in three-electrode electrochemical set-up are performed afterwards [1]. With a relatively simple set-up in protein-film voltammetry, we can get plenty of relevant information about enzymes redox chemistry [1–7]. However, we must point out that experiments in protein film voltammetry still suffer from many troubles coming mainly from the very complex structure of enzymes. The major problem is the efficient “reachability” of the redox active

center of many redox enzymes that is commonly “hidden” deeply in the protein tertiary structure. In many redox enzymes, the bulky polypeptide backbones hinder an efficient electron exchange between the working electrode and the redox active center of given adsorbed redox enzyme [1,6,7]. This drawback in protein-film voltammetry has been overcome by modifications of working electrode surface, mainly via adsorption of some conductive materials such as the nano-particles or with some redox mediators [1,5,7]. The redox active site of oxidoreductases (most common class of redox enzymes) is commonly an organic complex of some polyvalent metal transient cation (iron, copper, manganese, molybdenum) or a specific organic molecule [6]. From the organic molecules, the most common compounds acting as redox-active centers in the redox enzymes are quinones and flavins [1,6,7]. Under physiological conditions, many of the quinones act as a two-electron, two-proton redox centers [6,7]. In the sequence of their redox transformation, usually a semiquinone stable radical is often created. In this fashion, the redox chemistry of many quinones and hydroquinones is described with a two-step sequential (1

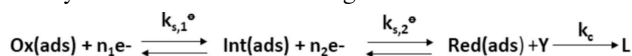
[a] P. Kokoskarova, V. Maksimova, M. Janeva, R. Gulaboski
Faculty of Medical Sciences, Goce Delcev University, Stip,
Macedonia
E-mail: rubin.gulaboski@ugd.edu.mk

electron-1 proton) redox reactions [6,7]. Similar scenarios are met in the redox chemistry of many polyvalent complexes of transient metal cations as explained in [1,2,6]. Although several experimental improvements by the protein-film voltammetry are reported in recent years, the theory of many enzymatic reactions under voltammetric conditions is far from over. This holds true especially for the theory of two-step electrode reactions of many redox enzymes under conditions of pulse voltammetric techniques. Although several theoretical models have been reported in the past decade related to the features of two-step electrode reactions under conditions of cyclic staircase voltammetry [1,7–12] and in square-wave voltammetry for systems with one and two electrode steps [13–30], yet there are still many new aspects emerging that need additional considerations. In this work we present results of a new theoretical model in square-wave voltammetry (SWV). We consider theoretically the features of two-step consecutive electrode reaction of adsorbed enzymes, whose electrochemically generated final product at the working electrode surface experiences irreversible chemical transformation. The electrochemical description of this particular mechanism is EECirr (i.e. Electrochemical-Electrochemical-Chemical_{irreversible}). As previously explained, justification for this redox mechanism is found in the chemistry of many redox enzymes that contain polyvalent cations of transient metals or quinone moiety as redox active sites in their structures. The sequential two step redox transformation of quinones to hydroquinones, for example, proceeds via formation of stable semiquinones intermediates. If the protonation steps in these sequences are fast, then the quinone to hydroquinone redox transformation in the lipophilic redox enzymes can be approximated to proceed as a surface EE reaction as explained in [1,5–7,18]. If an irreversible chemical transformation of created final hydroquinones in the physiological conditions can take place, then the entire mechanism can follow the principles of a surface EECirr mechanism. Indeed, an irreversible follow up chemical reaction coupled to the final reduction product of second electrode transformation, can often lead to a denaturation of given enzyme. However, as it has been recently shown [32–33], the enzymatic denaturation studied in square-wave voltammetry can be manifested via very specific features that can give us hints about enzyme stability. Moreover, in [32] we proposed simple and efficient methodology to get access to the kinetics of enzymatic denaturation. This, in turn, will provide relevant information about factors affecting enzyme activity in a given experimental set up. We chose the square-wave voltammetry as a working technique due to its unique features in gaining information for recognizing particular redox mechanism [23,26–31], but also because of its superiority in accessing thermodynamic and kinetic parameters from simple voltammetric experiments [23]. The results presented in this work are relevant to many lipophilic redox enzymes, but also to other lip-

ophilic organic compounds that can undergo sequential two step redox transformation from adsorbed state.

2. Mathematical Model

We consider theoretically a surface E₁E₂Cirr (or simply, EECirr) mechanism in protein-film square-wave voltammetry described with following reaction scheme:



The first electrode step assigned as E₁ comprises the following sequence: Ox(ads) + n₁e[−] ↔ Int(ads), while the second electrode step E₂ considers following sequence of this redox mechanism: Int(ads) + n₂e[−] ↔ Red(ads). The irreversible chemical step “Cirr” is coupled to the product of the second redox step, and it comprises following sequence of events: Red(ads) + Y → L.

Initially, only Ox species are present in adsorbed state at the surface of the working electrode. Int(ads) species are chemically stable adsorbed intermediates that are created as a result of reduction of Ox(ads) in the first electrode step. Red(ads) species are the final redox active species, created in the second electrode transfer step. By “Y” we define an electrochemically inactive compound (in the potential region used). Y can selectively react only with Red(ads) species, converting them to final electrochemically inactive product L. We assume that Y is present in large excess in electrochemical cell. Therefore, we suppose that the concentration of Y is constant at the electrode surface in the course of voltammetric experiment, so the irreversible chemical step at considered surface EECirr mechanism is of pseudo-first order. In the mathematical model, we assume that all redox active species are uniformly adsorbed on the electrode surface, while forming an electrochemically active monolayer. In addition, we assume that there is no mass transfer taking place by diffusion, and no-interactions of any kind occur between adsorbed molecules. The surface EECirr mechanism is solved under following conditions:

$$t = 0; \Gamma(\text{Ox}) = \Gamma^*(\text{Ox}); \Gamma(\text{Int}) = \Gamma(\text{Red}) = 0$$

$$t > 0; \Gamma(\text{Ox}) + \Gamma(\text{Int}) + \Gamma(\text{Red}) = \Gamma^*(\text{Ox})$$

for $t > 0$, the following conditions apply for the mechanism considered:

$$d\Gamma(\text{Ox})/dt = -I_1/(n_1FS)$$

$$d\Gamma(\text{Int})/dt = I_1/(n_1FS) - I_2/(n_2FS)$$

$$d\Gamma(\text{Red})/dt = I_2/(n_2FS) - k_c\Gamma(\text{Red})$$

We assume that a Butler-Volmer formalism of the interdependence between the electric current, applied potential, surface concentrations and the electrode reaction parameters holds at the working electrode surface

[23]. The recurrent formulas for calculating dimensionless currents Ψ of theoretical SW voltammograms as a function of the potential applied, incorporated in the corresponding MATHCAD file of this mechanism, are given in the *Supplementary material* of this work. In the recurrent formulas (I–IV) of the MATHCAD file given in Supplementary material, the reduction current is considered to be positive. The dimensionless currents are defined as $\Psi_I = I_1 / [(n_1 F S f T^*)]$ and $\Psi_{II} = I_2 / [(n_2 F S f T^*)]$, for the first and the second electrode step, respectively. In the last equation, I is symbol of electric current, n_1 and n_2 are the numbers of electrons exchanged between the working electrode and the corresponding redox active forms in the first and the second electrochemical step, respectively. We defined in all simulations that $n_1 = n_2 = n = 1$. By S we define the active electrode surface area, f is the SW frequency ($f = 1 / 2t_p$, where t_p is the duration of a single potential pulse in SWV) and T^* is the total surface concentration (i.e., the initial surface concentration of adsorbed Ox species). With Φ we define the dimensionless potential ($\Phi_1 = nF(E - E_1^\circ) / RT$ and $\Phi_2 = nF(E - E_2^\circ) / RT$, where E_1° and E_2° are the standard (or more precisely, the formal) redox potentials of the first and the second electrode step, respectively. α is the electron transfer coefficient (we assumed that α was equal to 0.5 for both electrode transfer steps), T is thermodynamic temperature (T was set to 298 K in all simulations), R is the universal gas constant, and F is the Faraday constant. The overall dimensionless current of calculated SW voltammograms is defined as a sum of the currents of the first and the second electrode step, i.e. $\Psi = \Psi_I + \Psi_{II}$.

In the recurrent formulas of the MATHCAD file given in Supplementary material, there are three dimensionless kinetic parameters controlling the rate of electrode processes. The dimensionless electrode kinetic parameters $K_1 = k_{s,1}^\circ / f$ and $K_2 = k_{s,2}^\circ / f$ reflect the influence of formal rate constants of first and second electrode step $k_{s,1}^\circ$ and $k_{s,2}^\circ$ relative to the time duration of a given SW pulse (via the SW frequency) to the features of calculated SW voltammograms. On the other side, the dimensionless chemical kinetic parameter K_{chem} reflects the rate of the chemical step to the SWV responses. This parameter is defined as $K_{\text{chem}} = k_c / f$, where k_c is the first order rate constant of the follow up chemical step of the surface EECirr mechanism. The last parameter is defined as $k_c = k_c' c(Y)$, where k_c' is the real chemical rate constant, and $c(Y)$ is molar concentration of chemical agent Y present in voltammetric cell. M is a numerical integration factor defined as $M = \exp(K_{\text{chem}}(m/50)) - \exp(K_{\text{chem}}(m-1)/50)$, where m is the serial number of time intervals. If not otherwise stated, the parameters of applied potential were: SW frequency $f = 10$ Hz, SW amplitude $E_{\text{sw}} = 50$ mV, and potential step $dE = 4$ mV. More details of the algorithm used can be found in [24,31]. MATHCAD 14 commercial software was explored for performing all theoretical simulations. It is worth to note that all the potentials of the simulated voltammograms are referred vs. the standard redox potential of the first electrode step

E° . If not otherwise stated, the SWV peak appearing at more positive potentials is that of the first electron transfer step at working electrode surface. In all cases, the starting potential is set to positive values and it runs toward final negative potentials.

3. Results and Discussions

As the features of calculated square-wave voltammograms at all two steps electrode mechanisms strongly depend on the potential difference between the standard redox potentials (i.e. the energy difference) of the two electron electrode reactions [7,17,18,20,22,30], we discuss in this work two different situations in that respect. In first scenario, we elaborate the features of calculated SW voltammograms when the energy of occurring of second electrode step is at least -150 mV or more negative than that of a first electrode step of the two-step surface EECirr mechanism. In such sequence of events, we commonly observe two peaks, which are clearly separated on potential scale. The second situation is the one in which the standard redox potential of the second electrode step is more positive or equal to that of the first electrode step. In such scenario, only one SW voltammetric signal is observed, hiding in its shape the features of both electrode steps, and the influence of the rate of chemical reaction, too. Obviously, the last situation can be quite complex and it requires more aspects to be considered in order to get correct explanations of the voltammetric features observed.

3.1 A. Situation of Two SW Voltammetric Peaks of Both Electrode Steps Separated for at Least -150 mV on Potential Scale

When energy needed for occurrence of second electrode step is -150 mV or more negative than that of the first electrode step, then we observe well-separated SW voltammetric peaks. Under such conditions, it is crucial to investigate the features of calculated SW voltammograms as a function of rate of follow up chemical reaction. Indeed, this effect is important to be considered in case of both, moderate and fast electron transfer reactions featured at both electrode steps. Shown in Figure 1 are SW voltammograms calculated for slow-to-moderate rates of electron transfer of both electrode steps ($K_1 = K_2 = 0.5$) and for several values of chemical rate parameter K_{chem} .

As the rate of chemical step increases from K_{chem} of 0.00001 to 0.05, we observe a decrease of all current components of the second SWV peak (i.e. the SW peak at more negative potentials). As K_{chem} gets values bigger than 0.05, then we see no further effect of K_{chem} to the SWV voltammetric outputs. This behavior of the second SWV peak (at more negative potentials) is typical as that of one-step surface ECirr reaction described in [22,23,32,33]. Note that the first SWV signal (at more positive potentials) is insensitive of K_{chem} under such circumstances. However, more complex scenario exists if

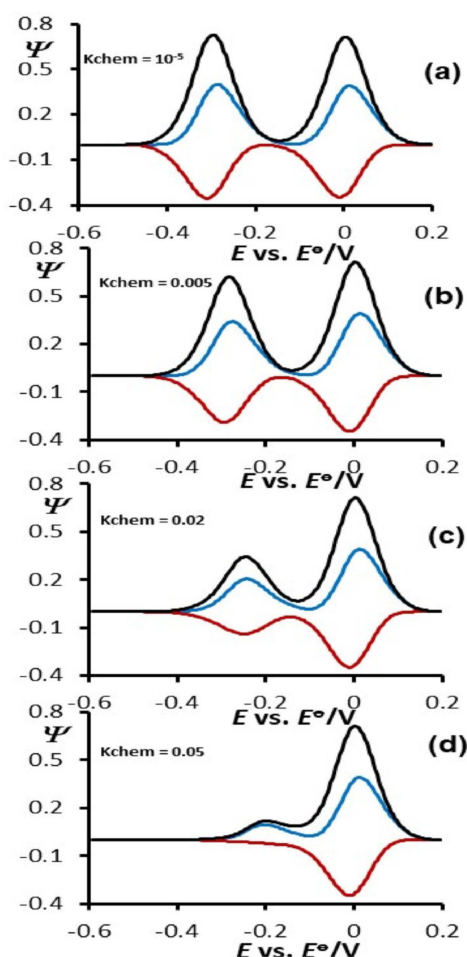


Fig. 1. Surface EECirr mechanism- Second electrode step occurs at potentials -15 mV or more negative than that of first electrode step: Effect of dimensionless chemical parameter K_{chem} to the features of calculated SW voltammograms in case of slow-to-moderate rate of electron transfer of both electrode steps ($K_1=K_2=0.5$). Other simulation parameters were: SW frequency $f=10$ Hz, SW amplitude $E_{\text{sw}}=50$ mV, potential step $dE=4$ mV, temperature $T=298$ K. In all simulations, value of electron transfer coefficients of first and the second electrode reaction was set to $\alpha=0.5$, and number of electron exchanged was $n_1=n_2=1$. Values of K_{chem} are given in the charts.

both electrode steps fall in the region of moderate-to-fast electron transfer.

Shown in Figure 2 is a series of SW voltammograms calculated in a wide range of rate of chemical parameter and for $K_1=K_2=1.78$ (i.e. region of moderate-to-fast electron transfer in both electrode reactions). In the region of K_{chem} from 0.00001 to 0.01 (Figure 2a–c) we observe that an increase of the chemical rate parameter is followed by an initial increase (and not by decrease) of all SW current components of the second peak positioned at more negative potentials. Moreover, we see that in this region of chemical reaction rates, the backward (i.e. the reoxidation) current components of second voltammetric peak at more negative potentials increase more intensively than the forward (reduction) SW peak currents.

This phenomenon is explained in more details in our recent theoretical works [32,33] and it is a consequence of specific chrono-amperometric features of this mechanism in SWV. In [32] we showed that the electrode transformation and the chemical reaction can occur in the whole time-segment of each potential SW pulse, and not exclusively in the time-measuring segment at the end of SW potential pulses. We have also shown that quite specific features in this mechanism happen at fast electrode reactions, when the chemical rate of conversion is comparable to the rate of electron transfer of second electrode step [32]. As demonstrated in [32], the irreversible chemical removal of the product of second electrode transfer step in so-called “dead-time” of each potential pulse in SWV gives an opportunity of more electrode active material to be available for electrode redox transformation at the end of the SW pulses. This material is additionally resupplied by the occurrence of first electrode step of a surface EECirr reaction. Eventually, after K_{chem} gets values bigger than 0.02 (Figure 2d–f), we observe features at second peak (at more negative potentials) that are typical of a surface redox reaction coupled with irreversible follow-up chemical step as described in [23,31,32]. It is worth to mention that in the region of $-2.5 < \log(K_{\text{chem}}) < -1.0$, the net SW peak potential of the second peak shifts for about +120 mV for every tenfold increase of K_{chem} . This finding is consistent as that reported previously for one-step surface ECirr mechanism [23]. Shown in Figure 3 is the dependence between the net SWV peak currents of the second electrode process as a function of $\log(K_{\text{chem}})$. The local maximum featuring in this “sigmoidal-like” curve appears in the region of $-3 < \log(K_{\text{chem}}) < -1$. As explained in [32,33], this phenomenon reflects the influence of rate irreversible follow-up chemical step to the kinetics of the second electrode reaction of surface EECirr mechanism. Indeed, the effect of K_{chem} to the chronoamperometric features to both reduction and reoxidation currents of the electrode process occurring at more negative potentials is crucial factor for phenomenon of net SWV peak increase observed at Figure 3.

In [32,33] it is reported that this feature is typical for surface electrode reactions that are coupled to follow up chemical step only. Therefore, this phenomenon can be explored as a diagnostic criterion for recognizing this particular electrode mechanism. In [32,33] we have also shown that the effect of the rate of irreversible follow-up chemical reaction to the SWV features of surface EC systems is more pronounced at fast electrode reactions. Shown in Figure 4a–i (panel A and panel B) is a series of calculated SW voltammograms, where the effect of rate of follow up chemical step is studied at fast electrode reactions of both electrochemical steps ($K_1=K_2=10$). Recognizable feature of surface electrode reactions exhibiting fast electrode reactions is a “splitting of the net SW voltammetric peak” and a sharp descending of measured peak currents [23,34–38]. An increased electron transfer rate between working electrode and the adsorbed redox

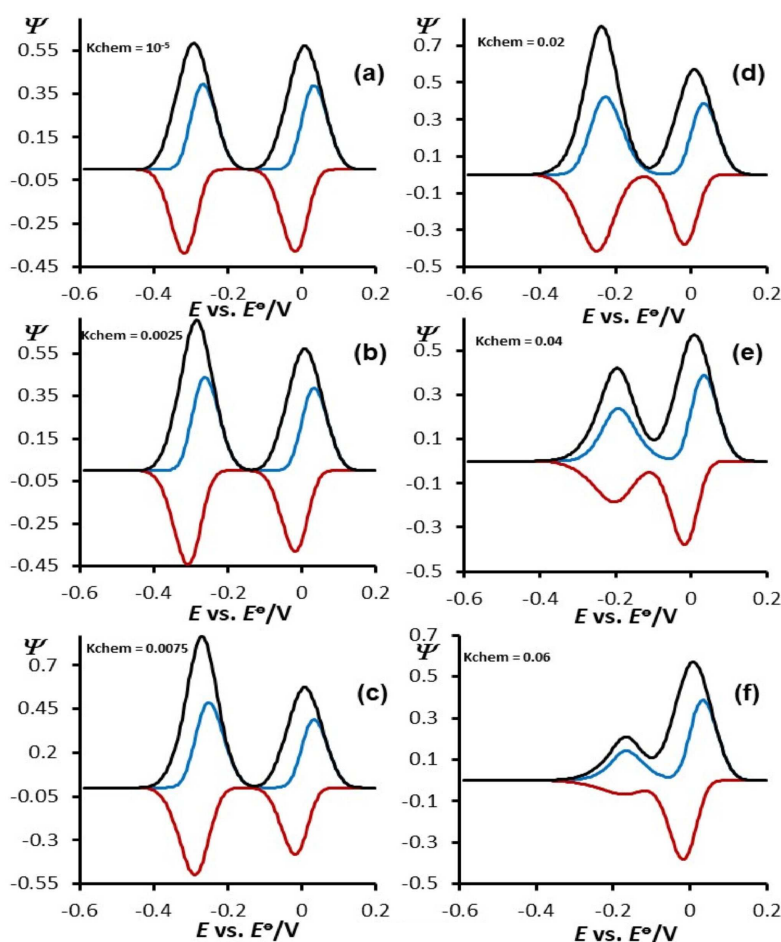


Fig. 2. Surface EECirr mechanism- Second electrode step occurs at potentials -150 mV or more negative than that of first electrode step: Effect of the dimensionless chemical parameter K_{chem} to the features of calculated square-wave voltammograms in case of moderate-to-fast rate of electron transfer in both electrode steps (i.e. $K_1=K_2=1,78$). All other simulation parameters were same as in Figure 1. The values of K_{chem} are given in the charts.

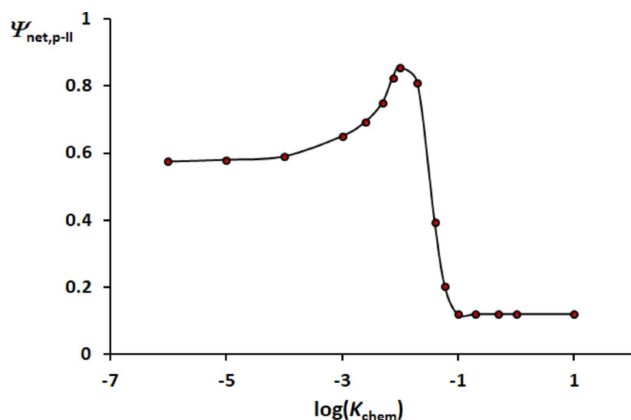


Fig. 3. Dependence of the net SW peak currents of second voltammetric peak (at more negative potentials) as a function of $\log(K_{\text{chem}})$. Other simulation parameters are same as in Figure 2.

active compounds leads to shifting of reduction peak potentials to more positive values, and that of re-oxidation peaks towards more negative values. Indeed,

less energy is required for both electrode processes to occur, as their kinetics gets bigger. A final output of these interplays at surface electrode processes is portrayed in “splitting of the net SWV peak” (Figure 4a). On the other side, if the electron transfer rate between the working electrode and the redox adsorbates is large, then a very short time is needed for the electrode transformation of oxidized to reduced form. Consequently, when the duration of a given SW potential pulse is longer than the time needed to achieve an electrode redox transformation of Ox(ads) to Red(ads), we get a very small current measured in the time-frame of current measurement at each SW pulse. This effect results in very small voltammetric currents measured, as it is shown in Figure 4a. Shown in Figure 4b–i is the influence of the rate of follow up chemical reaction to the features of “split net SW voltammograms” of a two-step surface EECirr mechanism. Compared to previous elaborated situation (see Figure 2), we recognize here at least four different moments appearing at the second voltammetric process positioned at more negative potentials: (1) The rate of

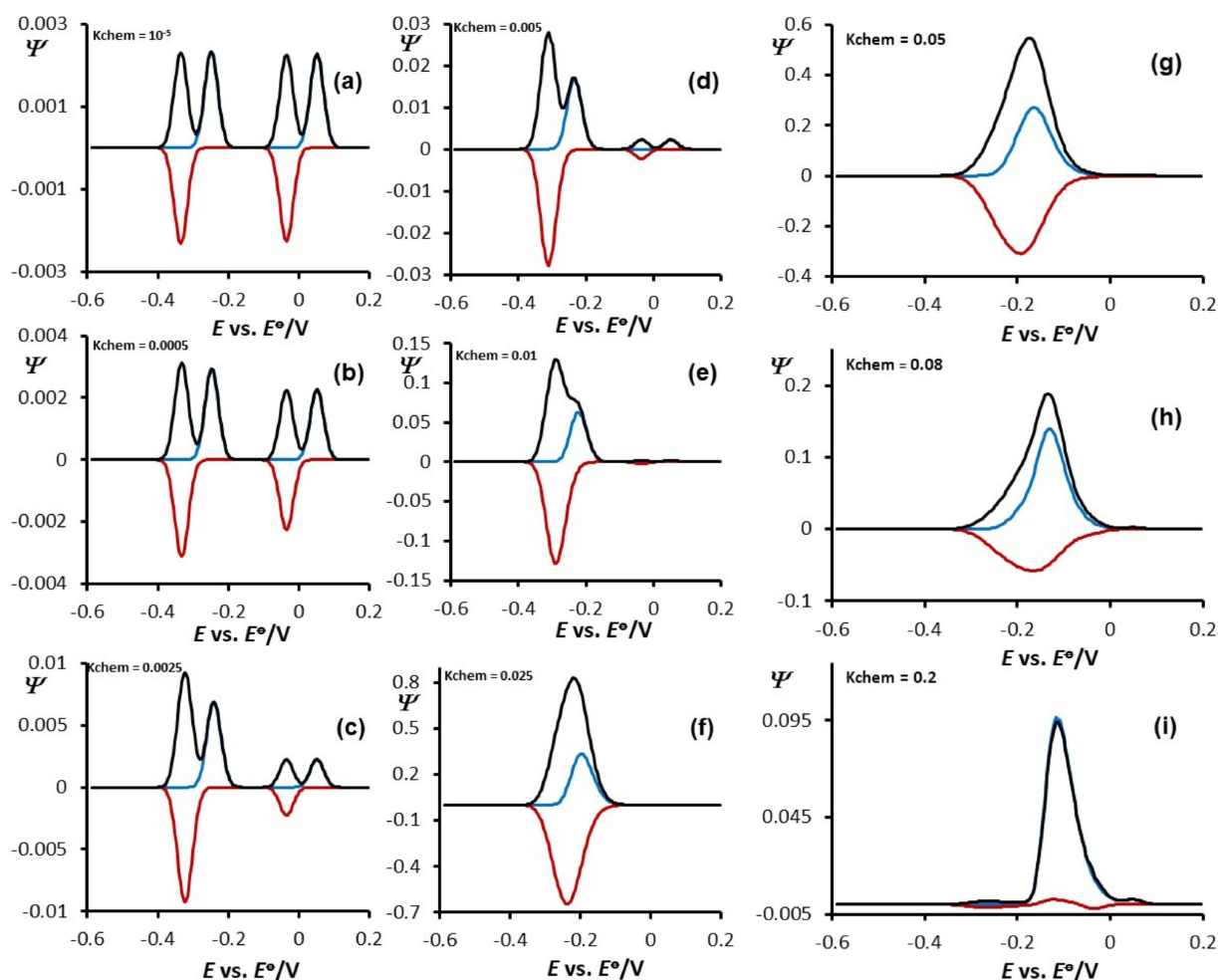


Fig. 4. Surface EECirr mechanism- Second electrode step occurs at potentials -150 mV or more negative than that of first electrode step: Effect of the dimensionless chemical parameter K_{chem} to the features of calculated square-wave voltammograms in case of fast rate of electron transfer at both electrode steps (i. e. $K_1=K_2=10$). All other simulation parameters were same as in Figure 1. The values of K_{chem} are given in the charts. Voltammograms in panel A are simulated for slow and moderate rates of irreversible chemical reaction, while voltammograms in panel B are simulated for significant rates of irreversible follow up chemical reaction.

irreversible chemical step starts to have an effect to the second electrode process at much smaller chemical reaction rates (see Figure 4b) than in the case of moderate electron transfer step (Figure 2b); (2) the intensity of increasing of backward (re-oxidation) SW peak current is much more pronounced in respect to the same effect at the forward (reduction) peak of the second electrode step; (3) As the rate of chemical reaction increases, the backward peak starts to shift to more positive potentials (Figure 4d–e). This phenomenon leads to eventual merge of the split net SWV peaks into a single net peak (see Figure 4f). In the region $0.01 < K_{\text{chem}} < 0.03$ we see very sharp increase of reoxidation over the reduction current component of the second electrode step (see Figure 4e–f and Figure 5). At Figure 5 we clearly see that the ratio between the backward vs forward peak currents on second electrode step shows a sharp maximum in the region of $-3 < \log(K_{\text{chem}}) < -1$. This is due to the effect of the rate of chemical step to the current features of this

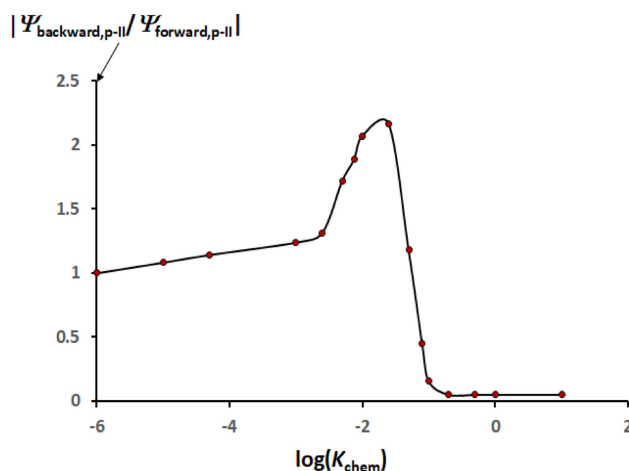


Fig. 5. Dependence of the ratios (absolute current values) of backward (reoxidation) vs forward (reduction) peak currents of second SW voltammetric peak as a function of $\log(K_{\text{chem}})$. Other simulation parameters are same as in Figure 4.

mechanism in SWV as described previously at Figures 2 and 3; (4) For values of $K_{\text{chem}} > 0.02$, the splitting of the net SWV peak of second electrode step disappears and we observe a single SW peak at more negative potentials (Figure 4f–i). A further increase of rate of irreversible chemical reaction (i.e. $K_{\text{chem}} > 0.03$) eventually leads to observing features typical for a surface ECirr reaction [32,33] at the second electrode process of a surface EECirr mechanism (Figure 4g–i). The phenomena portrayed in Figure 4 are unique for a surface ECirr reaction featuring fast electron exchange rate between the working electrode and the redox adsorbates [32,33]. Therefore, the phenomena shown in Figure 4 can serve as another criterion for recognizing a surface EECirr mechanism with fast electrode steps, in case of SWV peaks-separation for at least of -150 mV at potential scale between the second and the first SW peak. At this point, it is worth to point out that if second electrode step of surface EECirr mechanism occurs at potentials that are at least -150 mV (or even more negative) than that of first electrode step, then we can apply successfully the methods elaborated in [23,34–42] and in [33] to get independent access to kinetics of both electron transfer steps, as well as to the rate of the chemical step.

3.2 B. Situation of a Single SW Voltammetric Peak of a Surface Two-step EECirr Mechanism

This situation appears when the energy needed for the second electrode step of an EECirr mechanism is less or equal than that of the first electrode step. Under such circumstances, we observe a single SW voltammetric output appearing at potentials defined of the first electrode process. Indeed, in the shape of such a single SW voltammogram we find incorporated the features of both electrode steps, and the effect of the rate of chemical step, as well. Obviously, such an event is very difficult to be interpreted. This is due to the various interplay between the kinetic parameters of the first and the second electrode step, which get additionally complicated by different rates of follow-up irreversible chemical step. We try in this work to evaluate several scenarios, and to understand the effect of rate of chemical reaction to the SW voltammetric outputs, calculated at several different kinetics of the first and the second electrode step. Shown in Figure 6 are SW voltammograms of a surface EECirr mechanism, featuring moderate-to-fast rate of electron transfer reactions at both electrode steps ($K_1 = K_2 = 1.778$, and $E^\circ_1 = E^\circ_{\text{II}}$). As the value of chemical rate parameter increases from $K_{\text{chem}} = 0.000001$ to $K_{\text{chem}} = 0.05$, we see slight increase of all current branches, with more pronounced increase of the reoxidation (backward) peak current (Figure 6a–d). A further increase of the chemical rate parameters (for $K_{\text{chem}} > 0.08$) leads to slight decrease of all SWV current peaks, while reaching a steady-state situation for $K_{\text{chem}} > 0.2$ that produces SW voltammograms insensitive to further increase of K_{chem} (Figure 6e–f). Obviously, under such circumstances we observe a minute

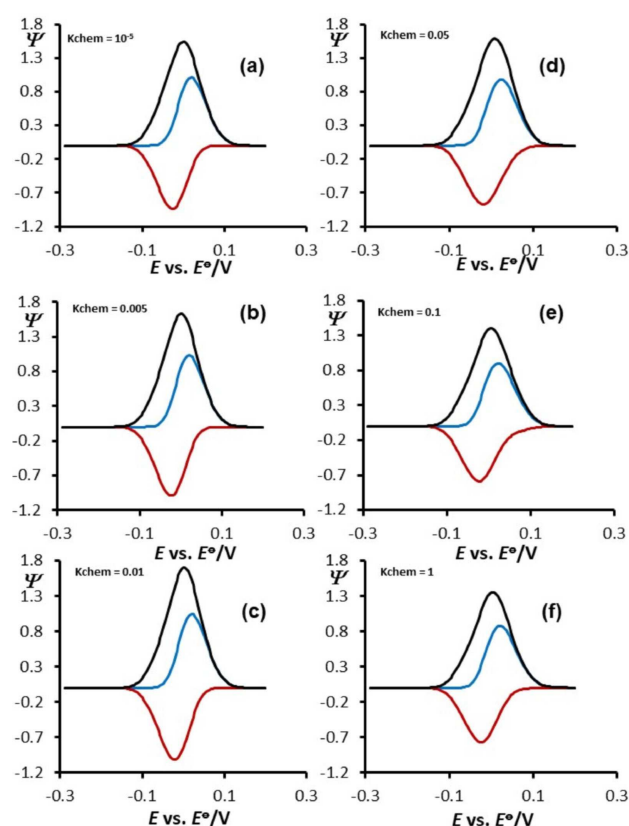


Fig. 6. Surface EECirr mechanism- Second electrode step occurs at potentials equal or more positive than that of first electrode step (i.e. $E^\circ_1 = E^\circ_{\text{II}}$): Effect of the dimensionless chemical parameter K_{chem} to the features of calculated square-wave voltammograms in case of moderate-to-fast electron transfer in both electrode steps (i.e. $K_1 = K_2 = 1.78$). All other simulation parameters were same as in Figure 1. The values of K_{chem} are given in the charts.

effect of chemical rate of follow up step to the features of calculated SW voltammograms. This is because the dominating resupply of electroactive material for second electrode reaction comes from the first electrode step, which occurs in this situation at the very same potential as the second one. That is why we observe a very small effect of K_{chem} to the features of only SW voltammetric peak existing under conditions defined. Indeed, more complex phenomena are met when we consider the effect of the chemical reaction rate to voltammetric characteristics of split net SWV peak.

Presented in Figure 7 is the effect of K_{chem} to the features of calculated SW voltammograms in situation of a split single net SW peak, which hides features of both electrode steps in it (voltammograms are simulated for $K_1 = K_2 = 10$, and $E^\circ_1 = E^\circ_{\text{II}}$).

As the effects observed at smaller values of K_{chem} in this situation (see Figure 7a–c) resemble to those shown in Figure 4, we see a fundamental difference if K_{chem} gets values larger than 0.05 (see Figure 7d–f). In such scenario, we again observe that K_{chem} affects all forward, backward and the net SW current components in region $0.001 <$

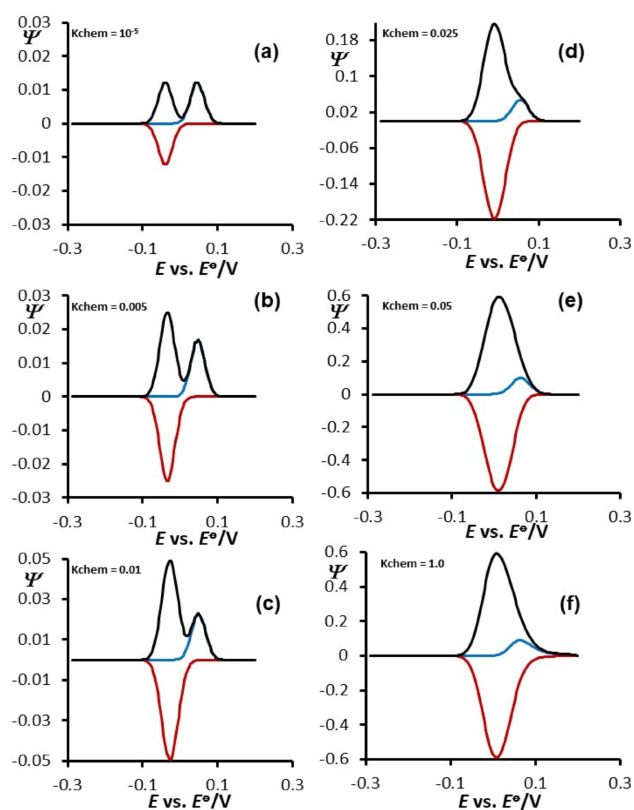


Fig. 7. Surface EECirr mechanism- Second electrode step occurs at potentials equal or more positive than that of first electrode step (i. e. $E_1^0 = E_2^0$): Effect of the dimensionless chemical parameter K_{chem} to the features of calculated square-wave voltammograms in case of fast rate of electron transfer in both electrode steps (i. e. $K_1 = K_2 = 10$). All other simulation parameters were same as in Figure 1. The values of K_{chem} are given in the charts.

$K_{\text{chem}} < 0.05$. If $K_{\text{chem}} > 0.05$, a steady-state SW voltammograms are observed with measurable forward and backward peak current components, regardless the value of K_{chem} . Interestingly, the reoxidation (backward) current component under such conditions remains much higher than the reduction (forward) SWV current component (Figure 7d–f). Moreover, the backward SW current component gets insensitive to K_{chem} , if $K_{\text{chem}} > 0.05$. This is quite different output than the features of SW voltammograms of one-step surface ECirr mechanism [32] (compare also Figure 7e–f and voltammograms in Figure 4f–i, for example). Therefore, this phenomenon can serve as additional qualitative criterion of distinguishing a surface two-step EECirr from a simple one-step surface ECirr mechanism, when both electrode processes of the EECirr mechanism occur at same potential. Two more interplays of the effect of K_{chem} to the features of calculated SW voltammograms are shown in Figures 8 and 9. In Figure 8, we can follow the effect of the rate of chemical follow up reaction, for $K_1 = 1.778$ (moderate rate of first electrode step) and $K_2 = 10$ (fast electrode second step). In such scenario, we observe a single SW voltammetric output that gains in intensity of all current components in the

region $0.005 < K_{\text{chem}} < 0.10$ (see voltammograms 8a–d). It is worth to mention that the reoxidation (backward) peak current increases more intensively than the reduction (forward) one by increasing K_{chem} . For values of $K_{\text{chem}} > 0.1$ we observe a steady-state SW voltammograms insensitive of further increase of K_{chem} (Figure 8e–f). Interestingly, if the first electrode step is very fast ($K_2 = 10$) and the electron transfer rate of the second electrode step is moderate-to-fast ($K_1 = 1.778$) (see Figure 9), we see a quite different SW voltammetric outputs than those presented in Figure 8. In such sequence of events, we observe a minute increase of all SWV current components up to of $K_{\text{chem}} = 0.02$ (Figure 9a–c). A further increase of the rate of chemical step of K_{chem} from 0.02 to 0.1 is followed by a decrease of all SWV current components (Figure 9d–e). Eventually, a steady-state SW voltammogram is reached for $K_{\text{chem}} > 0.1$, whose features are insensitive of K_{chem} (Figure 9e–f). The features elaborated at Figures 8 and 9 can serve as additional qualitative criteria to distinguish a two-step surface EECirr mechanism (when both electrode steps occur at same potential) from the simple surface ECirr mechanism (compare Figures 8 and 9, and Figures 1 and 2, for example). Moreover, the different characteristics of SW voltammograms portrayed in Figure 8 and Figure 9, might help to make a rough deduction about the kinetics of first and the second electrode step, too.

4. Conclusions

Although there are many redox lipophilic enzymes, acting under physiological conditions in a consecutive two-electron fashion [6], yet the theory of such systems studied under conditions of pulse voltammetric techniques in so-called “protein-film voltammetry” scenario is far from over. Several theoretical models have been already developed in the past two decades, related mainly to explain the features of lipophilic redox enzymes under conditions of cyclic staircase voltammetry and square-wave voltammetry [9–23]. In this work we present results of a theoretical model considering two-step consecutive electrode reaction of uniformly adsorbed redox enzymes coupled with irreversible chemical step of final electrode product in square-wave voltammetry. We assume that the electrochemically generated product of the second electrode reaction in this two-step mechanism gets further converted to an electrochemically inactive product via follow-up chemical reaction. The electrochemical description of this model is a surface EECirr mechanism. As we have shown in this work, for the two-step surface electrode processes complicated with irreversible follow up chemical reaction, successful evaluation of relevant kinetic parameters of both the electrode steps, as well as the kinetics of the chemical step, can be achieved only if the both electrode steps are separated for at least -150 mV at potential scale. Indeed, this holds true only for moderate rates of the kinetics of chemical step. In case of very high rates of follow up chemical reaction, the

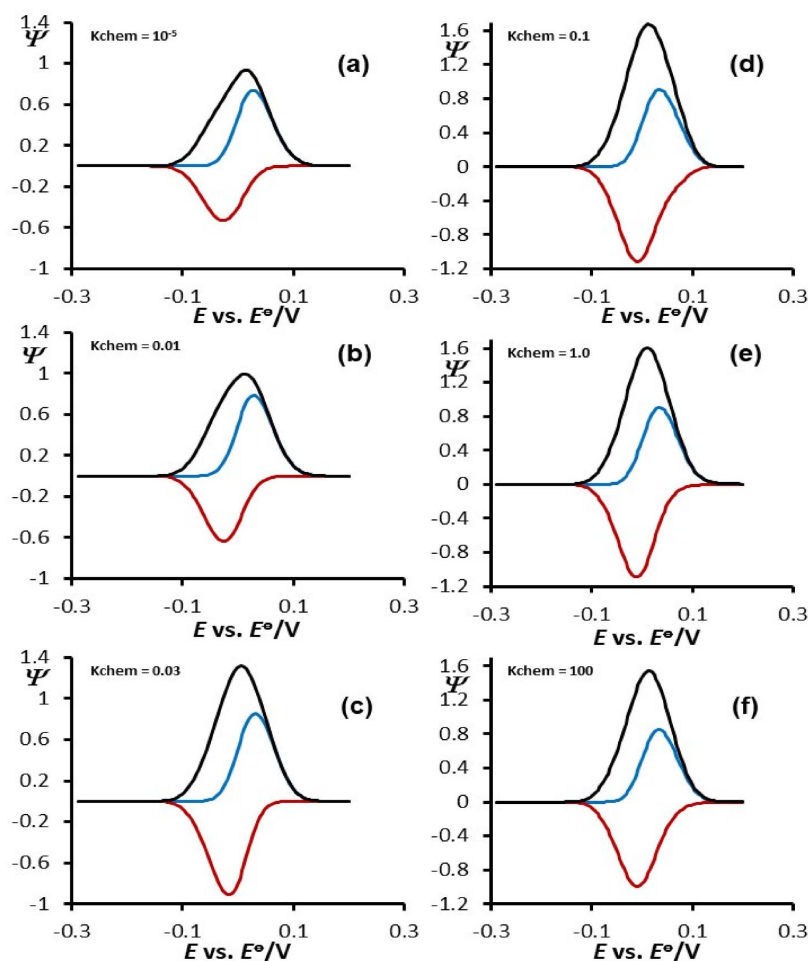


Fig. 8. Surface EECirr mechanism- Second electrode step occurs at potentials equal or more positive than that of first electrode step (i. e. $E^{\circ}_I = E^{\circ}_{II}$): Effect of the dimensionless chemical parameter K_{chem} to the features of calculated square-wave voltammograms in case of moderate rate of electron transfer in first electrode step ($K_1=1.78$) and fast rate of electron transfer in second electrode step ($K_2=10$). All other simulation parameters were same as in Figure 1. The values of K_{chem} are given in the charts.

peak potential of second electrode step can even overlap with the peak of the first electrode step at more positive potentials. Therefore, in such a scenario, the very large chemical reaction rates can make additional complications when attempts are made to determine kinetic parameters of a given enzymatic system. While the methods of “quasireversible maximum” [23] and the “split net SW peaks” [34] can be explored to get insight to the kinetics of the first electrode step of a surface EECirr mechanism, these methodologies are not suitable for the second electrode step. Since the second electrode step is coupled with a chemical irreversible reaction, the variation of the SW frequency (or the time) gives complex voltammetric patterns. This is because the SW frequency influences simultaneously both, the kinetics of the second electrode step, but also the rate of the follow-up chemical reaction. To avoid a complex interplay of kinetic parameters that can happen by varying the SW frequency, there is a better way to get insight to kinetics of electrode step of the second process, and to kinetics of follow-up chemical step, too. For this, we propose readers to explore method-

ologies elaborated in our recent works [32,33], where relevant information can be obtained only by varying the concentration of chemical agent Y at a constant scan rate. Indeed, when both electrode steps occur at the very same potential, there is a very complex SW voltammetric output to be elaborated. In such situation, a single SW voltammetric response is observed, hiding in its shape the features of both electrode steps, but also the influence of the follow up chemical step, too. In this work, we propose a simple method to distinguish the two step surface EECirr mechanism from a simple surface ECirr mechanism. This can be achieved in simple voltammetric experiments performed by varying the concentration of the chemical agent Y only, and observing the features of the SW voltammograms elaborated in Figures 6 to 9. Moreover, in such scenario, we also give hints for rough assessment of the kinetics of both electrode steps, too (see Figure 6 to 9). Indeed, to make a complete evaluation of all kinetic parameters of a surface EECirr mechanism, when both electrode steps occur at a very same potential, one needs more complex algorithm, as elaborated in [43–

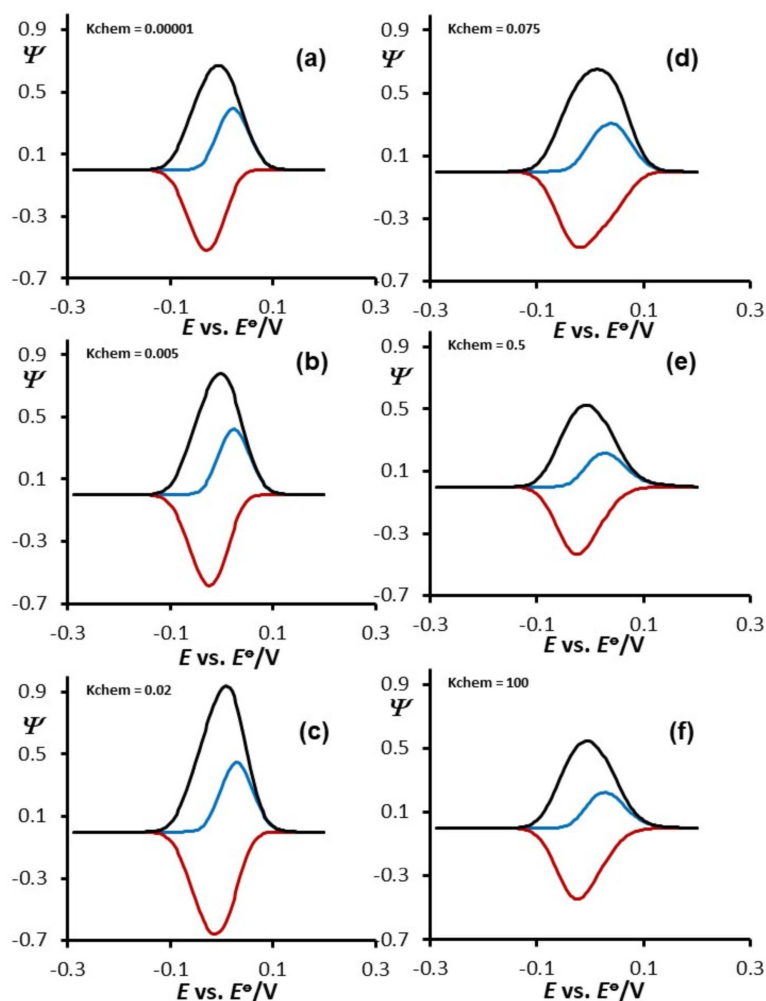


Fig. 9. Surface EECirr mechanism- Second electrode step occurs at potentials equal or more positive than that of first electrode step (i. e. $E^{\circ}_1 = E^{\circ}_{11}$): Effect of the dimensionless chemical parameter K_{chem} to the features of calculated square-wave voltammograms in case of fast rate of electron transfer in first electrode step ($K_1 = 10$) and moderate rate of electron transfer in second electrode step ($K_2 = 1.78$). All other simulation parameters were same as in Figure 1. The values of K_{chem} are given in the charts.

45]. At this point, it is worth to mention that the criteria we gave in this work for recognizing a two-step surface EECirr mechanism can efficiently distinguish it from similar two-step surface mechanisms, as the two-step surface EE mechanism [20,21] two-step surface ECE mechanism [22] and two-step surface catalytic EEC' mechanism [18]. In our further work, we gonna present theoretical results of a two-step surface electrode reaction that is coupled with reversible chemical step, and we will provide more relevant information about getting insight into kinetic and thermodynamic parameters of surface EEC mechanisms.

Acknowledgements

Rubin Gulaboski, Milkica Janeva and Viktorija Maksimova thank the “Goce Delcev” University Stip for the support via University founded project. All authors thank Professor Valentin Mirceski from Faculty of Natural

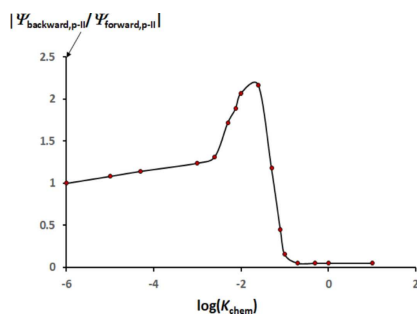
Sciences and Mathematics of “Ss Kiril and Metodij” University in Skopje, Macedonia, for his useful discussions.

References

- [1] F. A. Armstrong, *Electrifying metalloenzymes in: Metalloproteins: Theory, calculations and experiments* (A. E. Cho, W. A. Goddar III, eds). CRC Press, Taylor&Francis Group, London, New York, **2015**.
- [2] F. A. Armstrong, *Voltammetry of proteins. in: Encyclopedia of electrochemistry* (A. J. Bard, M. Stratmann, G. S. Wilson, eds), vol. 9, Wiley VCH, Weinheim, **2002**.
- [3] F. A. Armstrong, *Applications of voltammetric methods for probing the chemistry of redox proteins In: Bioelectrochemistry: Principles and practice* (G. Lenaz, G. Milazz eds), vol. 5, Birkhauser Verlag AG, Basel, **1997**.
- [4] F. A. Armstrong, H. A. Heering, J. Hirst, *Chem. Soc. Rev.* **1997**, 26, 169.
- [5] C. Leger, P. Bertrand, *Chem. Rev.* **2008**, 108, 2379.

- [6] P. N. Barlett, *Bioelectrochemistry: Fundamentals, experimental techniques and application*, Wiley, Chichester, **2008**.
- [7] R. Gulaboski, V. Mirceski, I. Bogeski, M. Hoth, *J. Solid State Electrochem.* **2012**, *16*, 2315.
- [8] R. Gulaboski, P. Kokoskarova, S. Petkovska, *Croat. Chem. Acta* **2018**, *91*, 377.
- [9] R. Gulaboski, P. Kokoskarova, S. Mitrev, *Electrochim. Acta* **2012**, *69*, 86.
- [10] C. Leger, S. J. Elliott, K. R. Hoke, L. J. C. Jeuken, A. K. Jones, F. A. Arsmtrong, *Biochem.* **2003**, *42*, 8653.
- [11] A. Molina, C. Serna, M. López-Tenés, M. M. Moreno, *J. Electroanal. Chem.* **2005**, 576, 9.
- [12] J. Galvez, R. Saura, A. Molina, T. Fuente, *J. Electroanal. Chem.* **1982**, *139*, 15.
- [13] M. Lovrić, *J. Electroanal. Chem.* **1983**, *153*, 1.
- [14] J. Galvez, M. L. Alcaraz, S. M. Park, *J. Electroanal. Chem.* **1989**, *266*, 1.
- [15] M. Lovric, S. Komorsky-Lovric, *Intern. J. Electrochem.* **2012**, <https://doi.org/10.1155/2012/596268>.
- [16] V. Mirceski, R. Gulaboski, *Maced. J. Chem. Chem. Eng.* **2014**, *33*, 1.
- [17] V. Mirceski, R. Gulaboski, M. Lovric, I. Bogeski, R. Kappl, M. Hoth, *Electroanalysis* **2013**, *25*, 2411.
- [18] R. Gulaboski, L. Mihajlov, *Biophys. Chem.* **2011**, *155*, 1.
- [19] E. Laborda, J. Gonzales, A. Molina, *Electrochim. Acta* **2014**, *43*, 25.
- [20] V. Mirceski, R. Gulaboski, *Croat. Chem. Acta* **2003**, *76*, 37.
- [21] J. J. O'Dea, J. G. Osteryoung, *Anal. Chem.* **1993**, *65*, 3090.
- [22] R. Gulaboski, *J. Solid State Electrochem.* **2009**, *13*, 1015. Supplementary Material: <https://link.springer.com/article/10.1007/s10008-008-0665-5>.
- [23] V. Mirceski, S. Komorsky-Lovric, M. Lovric, *Square-wave voltammetry: Theory and application*, (Scholz, F., Ed.) 2 ed., Berlin, Springer, **2007**.
- [24] R. Gulaboski, M. Lovric, V. Mirceski, I. Bogeski, M. Hoth, *Biophys. Chem.* **2008**, *137*, 49.
- [25] R. Gulaboski, M. Lovric, V. Mirceski, I. Bogeski, M. Hoth, *Biophys. Chem.* **2008**, *138*, 130.
- [26] A. Molina, J. Gonzales, *Pulse voltammetry in physical electrochemistry and electroanalysis, in Monographs in electrochemistry* (F. Scholz, ed.), Berlin Heidelberg, Springer, **2016**.
- [27] R. G. Compton, C. E. Banks, *Understanding voltammetry*, 2nd Edition, Imperial College Press, London, UK, **2011**.
- [28] A. J. Bard, L. R. Faulkner, *Electrochemical methods. Fundamentals and applications*, 3rd edition, John Wiley & Sons, Inc. **2004**.
- [29] J. G. Osteryoung, J. J. O'Dea, *Square-Wave Voltammetry, Electroanalytical chemistry: a series of advances*. Marcel Dekker, Inc: New York, **1986**.
- [30] A. B. Miler, R. G. Compton, *J. Phys. Chem. B* **2000**, *104*, 5331.
- [31] V. Mirceski, R. Gulaboski, I. Kuzmanovski, *Bull. Chem. Technol. Macedonia* **1999**, *18*, 57.
- [32] R. Gulaboski, *Electroanalysis* **2019**, *31*, 545.
- [33] R. Gulaboski, M. Janeva, V. Maksimova, *Electroanalysis* **2019**, *31*, <https://doi.org/10.1002/elan.201900028>.
- [34] V. Mirceski, M. Lovric, *Electroanalysis* **1997**, *9*, 1283.
- [35] J. J. O'Dea, J. Osteryoung, R. A. Osteryoung, *Anal. Chem.* **1981**, *53*, 695.
- [36] R. Gulaboski, V. Mirceski, M. Lovrić, I. Bogeski, *Electrochem. Commun.* **2005**, *7*, 515.
- [37] R. Gulaboski, V. Mirceski, *Electrochim. Acta* **2015**, *167*, 219.
- [38] P. Song, A. C. Fisher, J. D. Wadhawan, J. J. Cooper, H. J. Ward, N. S. Lawrence, *RSC Adv.* **2016**, *6*, 70237.
- [39] V. Mirceski, E. Laborda, D. Guziejewski, R. Compton, *Anal. Chem.* **2013**, *85*, 5586.
- [40] V. Mirceski, D. Guziejewski, M. Bozem, I. Bogeski, *Electrochim. Acta* **2016**, *213*, 520.
- [41] C. Batchelor-McAuley, E. Katelhon, E. O. Barnes, R. G. Compton, E. Laborda, A. Molina, *ChemistryOpen* **2015**, *4*, 224.
- [42] V. Mirceski, D. Guziejewski, K. Lisichkov, *Electrochim. Acta* **2013**, *114*, 667.
- [43] C. Bonazzola, G. Gordillo, *Electrochim. Acta* **2016**, *213*, 613.
- [44] P. Dauphin-Durcharme, N. Arroyo-Curras, M. Kurnik, G. Ortega, H. Li, K. W. Plaxco, *Langmuir* **2017**, *33*, 4407.
- [45] D. Guziejewski, V. Mirceski, D. Jadresko, *Electroanalysis* **2015**, *27*, 67.

Received: April 10, 2019
Accepted: April 25, 2019
Published online on ■■, ■■



*P. Kokoskarova, V. Maksimova, M. Janeva, R. Gulaboski**

1 – 12

Protein-film Voltammetry of Two-step Electrode Enzymatic Reactions Coupled with an Irreversible Chemical Reaction of a Final Product—a Theoretical Study in Square-wave Voltammetry
